Slip rates on San Francisco Bay area faults from anelastic deformation of the continental lithosphere

Eric L. Geist and D. J. Andrews

U.S. Geological Survey, Menlo Park, California

Abstract. Long-term slip rates on major faults in the San Francisco Bay area are predicted by modeling the anelastic deformation of the continental lithosphere in response to regional relative plate motion. The model developed by *Bird and Kong* [1994] is used to simulate lithospheric deformation according to a Coulomb frictional rheology of the upper crust and a dislocation creep rheology at depth. The focus of this study is the long-term motion of faults in a region extending from the creeping section of the San Andreas fault to the south up to the latitude of Cape Mendocino to the north. Boundary conditions are specified by the relative motion between the Pacific plate and the Sierra Nevada - Great Valley microplate [*Argus and Gordon*, 2000]. Rheologic-frictional parameters are specified as independent variables, and prediction errors are calculated with respect to geologic estimates of slip rates and maximum compressive stress directions. The model that best explains the region-wide observations is one in which the coefficient of friction on all of the major faults is less than 0.15, with the coefficient of friction for the San Andreas fault being approximately 0.09, consistent with previous inferences of San Andreas fault friction. Prediction error increases with lower fault friction on the San Andreas, indicating a lower bound of $\mu_{SAF} > 0.08$. Discrepancies with respect to previous slip rate estimates include a higher than expected slip rate along the peninsula segment of the San Andreas fault and a slightly lower than expected slip rate along the San Gregorio fault.

1. Introduction

This paper addresses how slip rate is partitioned among branches of the San Andreas fault system in northern California. There are few regions in central and northern California where the San Andreas fault accommodates the entire relative tectonic motion between the Pacific plate and the Sierra Nevada block. Like many plate boundaries, long-term deformation is distributed along a network of faults and in the intervening regions between major faults. The velocity of the Pacific plate relative to the Sierra Nevada block is fairly well known [*Argus and Gordon*, 2000]. The partition of this velocity into slip rates on various faults and into continuum deformation off the faults is determined by the geometry of the fault system and by the rheology of the crust and upper mantle. The focus of this study is determining long-term slip and deformation rates, averaged over many earthquake cycles. The elastic stress changes of earthquakes and elastic reloading of the seismogenic crust will average out to zero over the long term. Therefore the long-term deformation we seek to model is entirely anelastic.

The lack of a significant local heat flow anomaly along the San Andreas fault [e.g., *Lachenbruch and Sass*, 1992], in addition to a near-orthogonal orientation of maximum compressive stress axes to the fault [*Mount and Suppe*, 1987; *Zoback et al.*, 1987], have led researchers to infer that the shear strength of the San Andreas fault is low. A large difference between the intrinsic friction coefficient of rocks measured in the laboratory and the apparent friction coefficient inferred for major faults would suggest that most of the relative plate motion would be realized as fault slip. The other effect that needs to be considered, however, is the presence of an asthenospheric window inferred from the anomalously high regional heat flow in central and northern California (≈ 80 mW/m^2, *Lachenbruch and Sass* [1980]), favoring distributed deformation throughout the region.

To model the long-term anelastic deformation of the continental lithosphere dissected by a network of faults, we use the finite element code developed by *Bird* [1989] and *Bird and Kong* [1994]. In the continuum (off faults), stress is determined as the minimum of that found from a ductile flow law and that from Coulomb yielding. Stress from the ductile flow law, effective in the

lower crust and in the mantle, depends nonlinearly on strain rate and decreases with increasing temperature. Stress in the upper crust is governed by Coulomb (frictional) yielding, which represents slip on cracks and minor faults that are not modeled explicitly. The continuum model is equivalent to a layer of sand over a viscous substrate. Faults, which may have a smaller coefficient of friction or higher pore pressure than the continuum, are introduced explicitly into the finite element grid as described by *Bird and Kong* [1994]. *Bird and Kong* [1994] demonstrated that the strength of major faults in California including the San Andreas fault is low, similar to the low fault strength inferred for subduction zones [*Bird*, 1978, 1996; *Geist*, 1996]. We estimate friction coefficients and calculate slip rates for major faults in the San Francisco Bay area in more detail than was presented in the larger regional study of *Bird and Kong* [1994]. In particular, we take advantage of recent deep geophysical surveys and paleoseismologic investigations that have been performed since the *Bird and Kong* [1994] study was published to allow us to better constrain the model of neotectonic deformation in northern California.

The anelastic modeling done here is quite different from elastic dislocation modeling, which is appropriate to represent change of stress from an earthquake. It is an inappropriate extension of such a model to represent long-term slip rates as elastic dislocations on a prescribed network of faults. For a constant rate of remote stressing, elastic dislocation slip rates have been compared to geologic slip rates [*Bilham and Bodin*, 1992]. Such modeling neglects the fact that stress off the faults, particularly in gaps between fault segments, will build up to values that exceed the fracture strength of the unfaulted material. In a variation of this model, *Ward* [1997] locally prescribes an interseismic stress rate that corresponds to geologically determined slip rates, for the purpose of calculating synthetic earthquake catalogues. Stress changes from a sequence of earthquakes are superimposed on the secular interseismic rate to then determine seismic slip patterns. Elastic dislocation theory provides a simple and tractable framework for such modeling. It is valid for the purpose of modeling synthetic seismicity, but the interseismic stress rate is not physical.

Over the long term the stress driving crustal deformation is constant. The appropriate boundary condition for a fault system is plate tectonic velocities, not a secularly increasing stress. Fault segments continue to slip at constant long-term average stress because anelastic deformation is occurring in the gaps between them, as well as in the viscous substrate beneath them.

The objective of this work is to model fault slip rates in northern California. A model which has a good fit to measured stress directions and measured geologic slip rates can reasonably be expected to provide a good interpolation of slip rate at points where it has not been measured.

2. Model Description

Bird's [1989] model of continuous deformation is derived by vertically integrating the Stokes equations of motion,

$$\frac{\partial \sigma_{ij}}{\partial x_j} + \rho g_i = 0, \quad i = 1, 2, 3, \tag{1}$$

numerically approximated using a Galerkin finite element technique with six-node isoparametric elements. Shear stress σ_s in the upper crust is given by a frictional, or Coulomb, rheology

$$|\sigma_s| \leq \mu(-\sigma_n - P_p), \tag{2}$$

where μ is the coefficient of friction and P_p is the pore pressure. Shear stress in the lower crust and mantle is given by a non linear creep rheology, dependent on the local geotherm

$$|\sigma_s| = A \left(2\sqrt{\Pi_e}\right)^{(1-n)/n} \exp\left(\frac{Q}{nRT}\right) e_s, \tag{3}$$

where A is the preexponential constant, Π_e is the second invariant of the strain rate tensor, n is the stress exponent ($n = 3$ for all cases in this study), Q is the activation energy, R is the gas constant, T is the temperature, and e_s is the shear strain rate. Horizontal gradients of vertical shear stress ($\partial\sigma_{13}/\partial x_1, \partial\sigma_{23}/\partial x_2$) are ignored in the equations of motion, such that vertical normal stress is lithostatic at all points. This assumption is quite likely valid in the tectonic environment of northern California where the effects of plate flexture and traction at the base of the lithosphere are small in comparison to the lateral balance of tectonic forces [cf., *Bird*, 1989; *Wdowinski et al.*, 1989; *Geist et al.*, 1993; *Ellis et al.*, 1995].

In an advance over previously developed thin viscous sheet models that parameterized lithospheric deformation using only a power law rheology [e.g., *England and McKenzie*, 1982; *Geist et al.*, 1993; *Geist and Scholl*, 1994], the model by *Bird* [1989] and following models are based on a combined Coulomb and power-law rheology. This nonlinear flow law is simulated in the finite element model by iteration of a linearized effective viscosity tensor. The main difficulty in incorporating deformation of the brittle upper crust into continuum models is that large matrix condition numbers arise from unbounded regions in the principal strain rate plane, defined by *Anderson*'s [1951] theory of faulting, being discontinuously mapped to the principal stress plane [*Houseman and England*, 1986]. Therefore a small amount of viscous compliance and judicious choices for iterating the effective viscosity tensor are needed by *Bird* [1989] to assure convergence of the iteration process.

Isoparametric curvilinear fault elements were introduced into the model by *Bird and Kong* [1994] by modifying the linearized stiffness matrix and forcing vector of the continuum model. For each fault element, frictional shear traction is calculated from the Mohr-

Coulomb friction law, and ductile shear traction is calculated from the width of the ductile shear zone, approximated by a quadratic function with depth in the lower crust [*Turcotte et al.*, 1980]. Heat production from narrow ductile shear zones such as those used in the *Bird and Kong* [1994] model is discussed by *Thatcher and England* [1998]. The friction coefficient for the faults (strictly, the apparent friction coefficient that includes pore pressure effects) is specified independently from the intrinsic friction of the continuum elements. Although fault dip is specified, the rake of the slip vector is calculated so as to minimize the vertically integrated shear traction at each fault element. Isostatic equilibrium, incompressibility, and other assumptions are given in the complete description of the model by *Bird* [1989] and *Bird and Kong* [1994].

2.1. Model Geometry

The finite element grid was constructed to include the major faults of the San Francisco Bay area shown in Figure 1. (Fault names are given in Plate 1a.) The side of a finite element is on average 10 km but varies considerably depending on the local fault geometry. Small continuum elements were used near faults to account for expected higher strain rates. As discussed below, the presumed fault geometry (strike, dip, continuity) has a large influence on the partitioning of slip. The surface traces of faults in the region were digitized from the *Working Group on Northern California Earthquake Potential (WGNCEP)* [1996] base map, using more detailed ancillary base maps where necessary. Evidence that these faults cut through to the lower crust is pro-
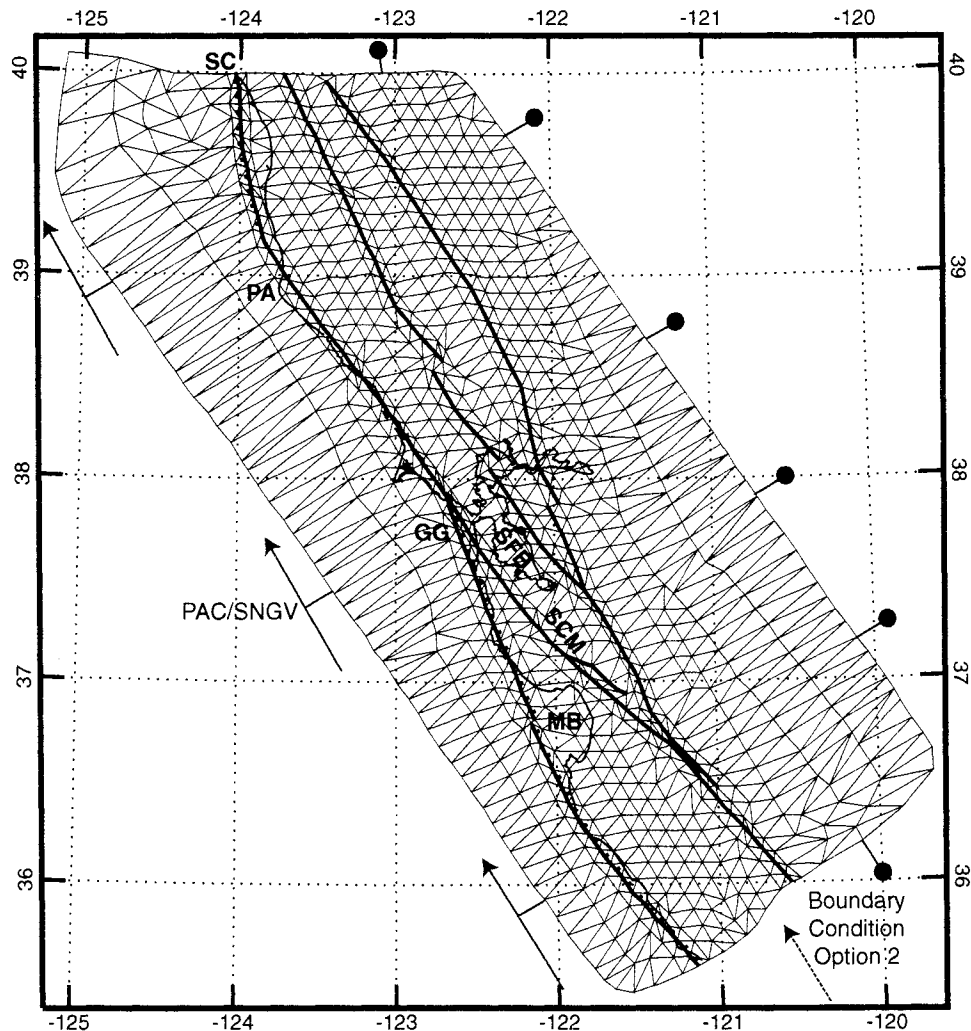
Figure 1. Finite element model grid and fault geometry. Velocity boundary conditions are specified along Pacific side of model according to the Pacific-Sierra Nevada pole of *Argus and Gordon* [2000]. Great Valley edge of model is held fixed. To match the slip rate along the creeping section of the San Andreas fault, velocity boundary conditions are specified along the southern edge of the model between the San Gregorio and San Andreas faults. (See Plate 1a for fault locations.) Geographic features: MB, Monterey Bay; SCM, Santa Cruz Mountains; SFB, San Francisco Bay; GG, Golden Gate; PA, Point Arena; SC, Shelter Cove; PAC/SNGV, Pacific plate-Sierra Nevada-Great Valley microplate relative velocity vector.

vided by regional seismicity [*Hill et al.*, 1991; *Zoback et al.*, 1999] and recent seismic refraction experiments [*Beaudoin et al.*, 1996; *Hole et al.*, 1998; *Parsons*, 1998]. The dip for all of the faults included in the model is 90° with the following exceptions: (1) a WSW dip of 74° for the offshore trace of San Andreas fault north of Point Arena, based on limited seismic reflection data and evidence for normal faulting in the region [*McCulloch*, 1987]; and (2) a NE dip of 65° for the San Gregorio fault (including the Sur and San Simeon segments to the south) based on seismicity and focal mechanisms in the region.

2.2. Nodal Parameters

Four nodal parameters are needed to calculate the vertically integrated stress through the lithosphere: elevation, crustal thickness, mantle lithosphere thickness, and heat flow. If we assume isostatic equilibrium, uniform heat production, and that the base of the lithosphere is an isothermal surface, only two of these parameters are independent. As with the *Bird and Kong* [1994] study, elevation is specified along with the heat flow field (C. Williams, personal communication, 1999) to specify the thickness of the crustal and mantle lithospheric layers. The resulting crustal thickness field closely matches the crustal thickness determined from seismic refraction data in the San Francisco Bay area by *Brocher et al.* [1994]; mantle lithosphere thickness ranges between 50 and 65 km. Because, under these assumptions, surface heat flow dictates the temperature distribution throughout the lithosphere, the data used in the model and to calculate lithosphere layer thicknesses do not include the Geysers heat flow anomaly (> 125 mW/m^2). Although *Bird and Kong* [1994] included the Geysers heat flow anomaly in their model, we choose not to include the anomaly as representative of the lithospheric geotherm in this region.

2.3. Boundary Conditions

The northeastern (Great Valley) edge of the model is fixed in two orthogonal directions, and a velocity boundary condition is applied along the southwestern (Pacific) edge of the model using the Pacific-Sierra Nevada angular velocity specified by *Argus and Gordon* [2000] (Figure 1). We test two possible ways the relative plate motion is applied to the San Andreas fault system. First, the Pacific-Sierra Nevada relative plate motion is applied strictly along the Pacific edge of the model with zero traction specified along the southern boundary between the San Gregorio-San Simeon fault and the creeping section of the San Andreas fault. For this option a large amount of motion is taken up along the San Gregorio-San Simeon fault with significantly lower than expected slip rates along the creeping section of the San Andreas fault (25-26 mm/yr compared to 32-34 mm/yr from the compilation of *Tse et al.* [1985]). The second option is to apply velocity boundary condi-

tions to the Pacific edge and also to the southern edge of the model between the San Gregorio and San Andreas faults (Figure 1). These boundary conditions, by necessity, give the correct San Andreas slip rate along the creeping section, with the consequence of lowering the slip rate along the San Gregorio fault. This second option is supported by the fact that the San Gregorio-San Simeon-Hosgri fault becomes less of a throughgoing structure to the south of the model domain as evidenced by seismicity [*Hill et al.*, 1991]. Therefore the second option is used for the models studied in Section 3.

2.4. Fault Friction

Although fault friction can be specified as an independent variable for each fault element, it is useful to introduce a constitutive relation to link long-term friction to a kinematic variable. Like *Bird and Kong* [1994], we specify that fault strength decreases with net slip along faults in the region (using values referenced in that paper), stemming from a mechanism proposed by *Byerlee* [1990] whereby hydraulic overpressure can be sustained in fault interiors and from observations that the thickness of fault gouge increases with slip [*Robertson*, 1982]. Decreasing long-term friction μ with respect to net slip D can be expressed as

$$\mu = \mu_0 \left(1 - \gamma \frac{D}{D_{\max}} \right) , \qquad (4)$$

where μ_0 is the friction coefficient for faults with zero net slip and γ is a fractional strength reduction factor. Thus friction coefficients will range from $\mu = \mu_0(1 - \gamma)$, for the master fault with the greatest net long-term slip (i.e., the San Andreas fault), to μ_0.

3. Results

To determine optimal rheologic parameters, a series of 48 experiments were run in which the parameters for fault friction (μ_0 and γ) and crustal activation energy in the lower crust were varied. An empirical relation based on the regional depth of seismicity is used to calculate A_{crust} from Q_{crust} [*Bird and Kong*, 1994]. For the present study, A_{mantle} and Q_{mantle} are held constant at 5.4×10^4 Pa s$^{1/3}$ and 457 kJ/mol, respectively [*Kirby and Kronenberg*, 1987]. Each experiment was scored by calculating the global root-mean-square prediction error with respect to observed geologic fault slip rates ($\epsilon_{\text{geologic}}$, Figure 2a) and weighted mean error with respect to principal compressive stress directions (ϵ_{stress}, Figure 2b), the weights corresponding to the quality grades (A-D) defined by *Zoback and Zoback* [1991]. Analysis of the stress data by *Bird and Kong* [1994] and *Bird* [1996] indicates that the local scatter (caused by measurement or sampling errors) has a standard deviation of approximately 17°. Thus the misfit of model stress predictions to the observed stress data will be at least 17°. Compared to the sensitivity of
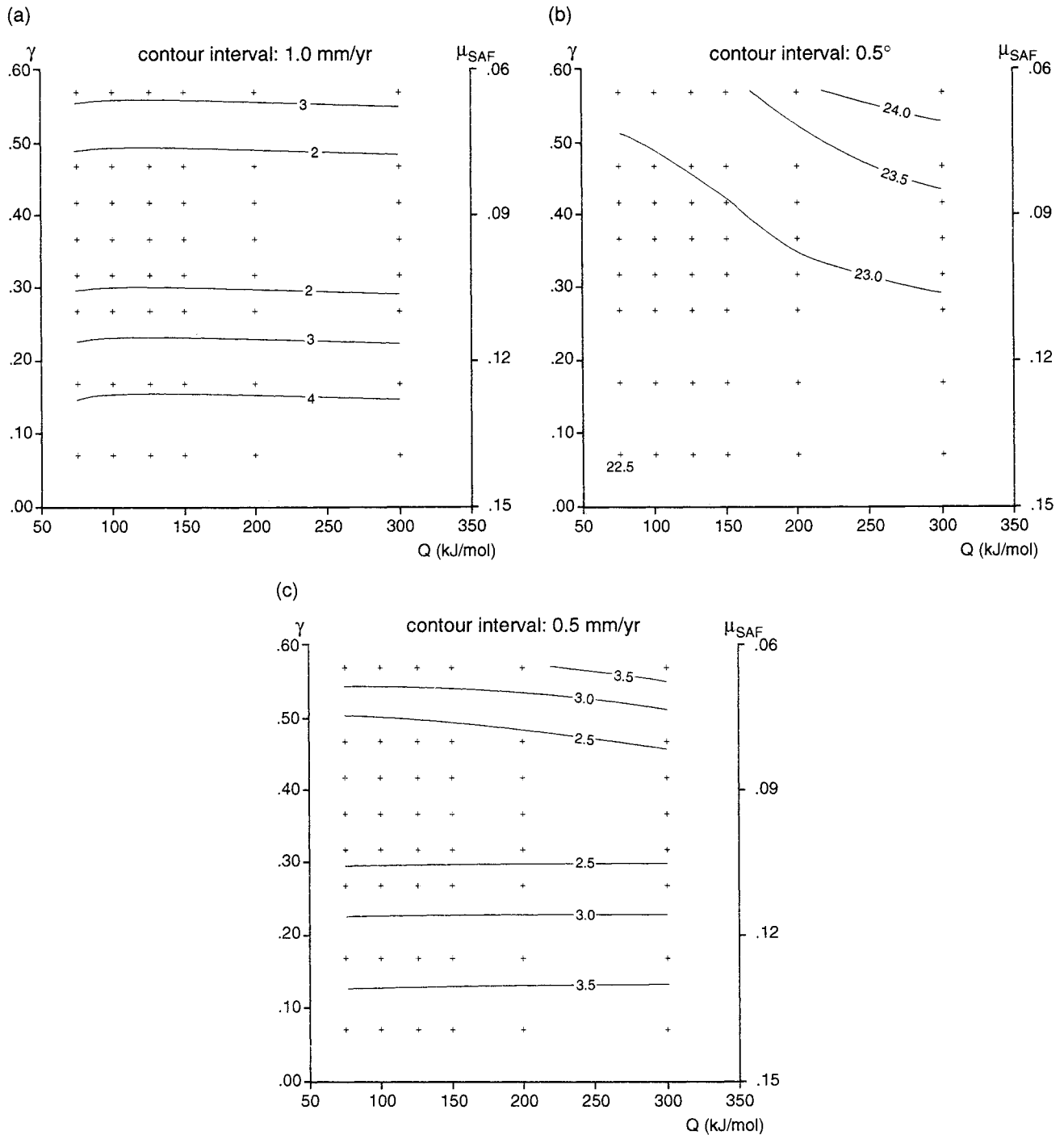
Figure 2. Prediction error of model results as a function of activation energy in the lower crust Q_{crust} versus the fractional strength reduction γ of major faults. Each cross represents a separate model run. (a) Prediction error calculated with respect to geologic slip rate observations (Table 1). Contour interval, 1 mm/yr. (b) Prediction error calculated with respect to maximum compressive stress directions. Contour interval, 0.5°. (c) Global prediction error calculated with respect to both geologic slip rate and stress direction data sets. Contour interval, 0.5 mm/yr.

model results with respect to geologic slip rate (Figure 2a), there is little variation ($< 2°$) with respect to principal stress orientations (Figure 2b). A global error (in mm/yr, Figure 2c) that combines the $\epsilon_{geologic}$ and ϵ_{stress} is calculated according to the following formula, consistent with *Bird and Kong* [1994]:

$$\epsilon_{global} \equiv \frac{1}{2} \left(\epsilon_{geologic} + \frac{\epsilon_{stress} - 17°}{2° \text{ yr/mm}} \right) . \qquad (5)$$

The geologic fault slip rates were compiled from published reports (Table 1), several of which are more recent than the *Bird and Kong* [1994] study. The stress

Table 1. Geologic Slip Rates Used to Score Models

Fault	Location	Slip Rate mm/yr	Reference
San Andreas	Shelter Cove	>14	*Prentice et al.* [1999]
San Andreas	Point Arena	<25 ± 3	*Prentice* [1989]
San Andreas	Olema	24 ± 3	*Niemi and Hall* [1992]
San Andreas	Filoli	17 ± 4	*Hall et al.* [1999]
San Gregorio	Año Nuevo	3-9	*Weber and Nolan* [1995]
San Simeon	San Simeon	1-1.4	*Hall et al.* [1994]
Hayward	Union City	8.0 ± 0.7	*Lienkaemper and Borchardt* [1996]
Rodgers Creek	Sonoma Mountain	>5.8	*Budding et al.* [1991]
Calaveras	Leyden Creek	5 ± 2	*Kelson et al.* [1996]
Concord	Galindo Creek	3.4 ± 0.3	*Borchardt et al.* [1999]

directions were obtained from *Zoback and Zoback* [1991] and supplemented with stress directions from 96 well-constrained focal mechanisms in the region [*Zoback et al.*, 1999]; (M. L. Zoback, personal communication, 1999).

The global prediction error of the model results indicates that there is little difference in the friction coefficient among major faults in the San Francisco Bay area (for $\mu_0 = 0.15$; $0.11 > \mu_{SAF} > 0.08$; Figure 2c). Prediction error is essentially insensitive to Q_{crust} for the range of friction coefficients tested. Therefore this study does not constrain the rheology below the upper crust. An optimal value of $\mu_{SAF} \approx 0.09$ is consistent with both the heat flow constraint ($\mu_{SAF} \leq 0.2$) and the constraint from the dominant principal compressive stress directions ($\mu_{SAF} \leq 0.1$) [*Lachenbruch and Sass*, 1992]. A lower bound on μ_{SAF} is suggested by the modeling results in which the global prediction error increases as μ_{SAF} decreases for values of μ_{SAF} below approximately 0.08 (Figure 2).

The model that fits both the geologic slip rates and stress directions with the minimum error is the one where $Q_{crust} = 100$ kJ/mol and $\mu_{SAF} = 0.094$ ($\gamma = 0.37$) (Plate 1a). There is generally good agreement on a segment-by-segment basis between the modeled slip rates and the slip rates assigned by *WGNCEP* [1996]. In particular, the 21-23 mm/yr rate for the San Andreas fault north of the Golden Gate, the 9 mm/yr rate for the Hayward fault, and the 15 mm/yr rate for the southern Calaveras fault all agree with the consensus rates in that report. Discrepancies, however, include a higher than expected rate (21-22 mm/yr compared to 17 mm/yr) for the Peninsula segment of the San Andreas fault and, perhaps, a lower than expected rate (2-3 mm/yr compared to 5 mm/yr) for the San Gregorio fault. The slip partitioning at the latitude of the San Francisco Peninsula determined by *Argus and Gordon* [2000] using their revised Pacific-Sierra Nevada Euler pole is in good agreement with our modeling results (21 mm/yr, San Andreas fault; 3 mm/yr, San Gregorio fault).

Fault geometry, along with fault friction, has a large influence on the model results. Whereas fault strike is well constrained from geologic mapping, fault dip through the crust is only known for seismically active faults or where deep geophysical experiments have been performed. Where fault dip is poorly constrained, it is necessary to examine what effect fault dip has on the local slip rate. For example, if we assume that the northernmost offshore segment of the San Andreas fault is vertical rather than dipping, the slip rate decreases to 13-14 mm/yr (marginally consistent with geologic observations at Point Arena and Shelter Cove, Table 1), with a concomitant slip rate increase on faults to the east that are more closely aligned with the relative plate motion. Conversely, if we assume that the dip from the source mechanism for the 1989 Loma Prieta earthquake [*Nábělek*, 1996] is representative for the Santa Cruz Mountain segment of the San Andreas fault, the slip rate increases to 29-34 mm/yr, with an attendant slip rate drop on the San Gregorio fault.

The other aspect of fault geometry that has a lesser effect on predicted slip rates is fault continuity. In general, slip rates vary only gradually within individual segments defined by fault intersections or step overs. In our model geometry we specified four major step overs between the following faults: Hayward-Rodgers Creek, Rodgers Creek-Maacama, Northern Calaveras-Concord, and within the San Gregorio fault at Monterey Bay. Other minor step overs in the fault traces are not considered, such that the faults are presumed to be continuous at depth. As slip rate decreases near fault terminations, there is locally distributed deformation through the step over regions. If the faults are continuous at depth for the large step overs, then the slip rates will be higher in these regions. The anelastic model presented here, however, indicates that fault continuity affects slip rates only in the vicinity of the step over. In contrast, *Bilham and Bodin* [1992] suggest, using an elastic model, that fault connectivity affects the slip rate on entire fault segments. Their elastic model predicts a crack-like scaling of slip rate with fault length. The underlying physics that dictates long-term slip rates is given by the anelastic (friction-dislocation creep) rheology of the continental lithosphere. For small segment lengths (less than approximately the scale of the up-
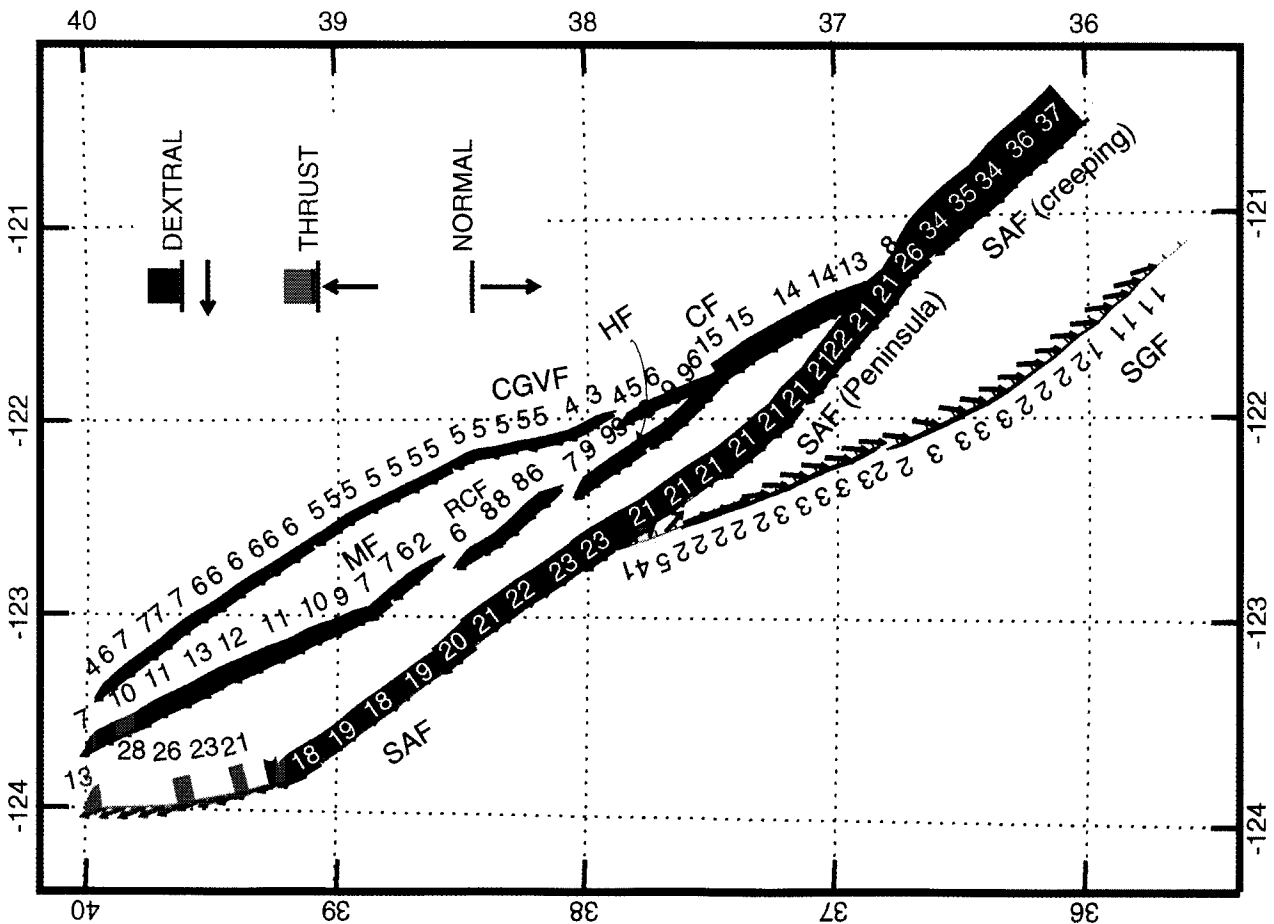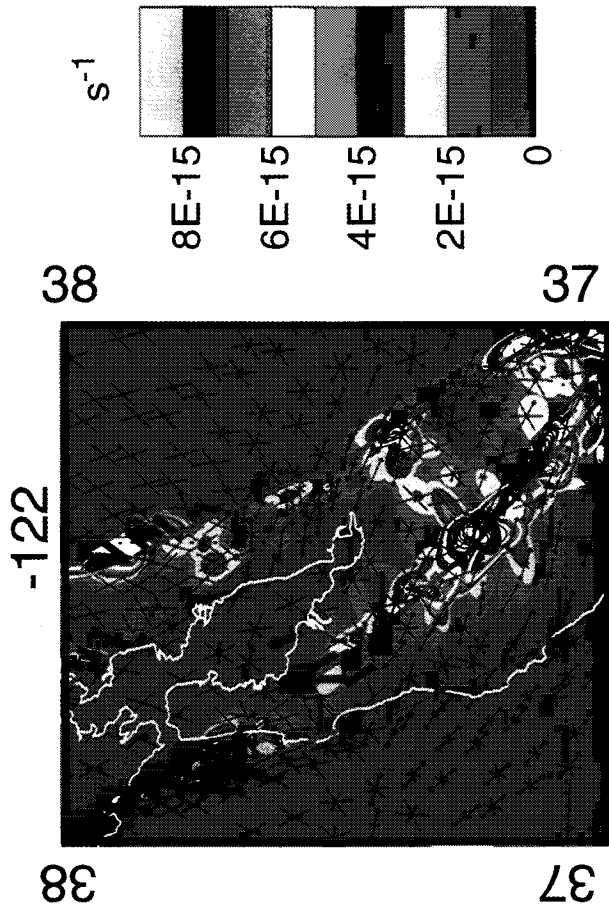
Plate 1. Results from model with minimum global error: $Q_{crust} = 100$ kJ/mol, $\gamma = 0.37$, $\mu_0 = 0.15$, $\mu_{SAF} = 0.094$. (a) Predicted slip rates along major faults. Numbers represent slip rate in mm/yr. Small arrows represent relative slip direction across fault. SAF, San Andreas fault; SGF, San Gregorio fault (including the Sur and San Simeon fault segments); HF, Hayward fault; CF, Calaveras fault; RCF, Rodgers Creek fault; MF, Maacama fault; CGVF, Concord/Green Valley fault. (b) Predicted maximum principal strain rate (color contours) and style of faulting (symbols) in the San Francisco Peninsula-Santa Cruz Mountain region. Symbols represent strikes of two possible faulting mechanisms at each location. Symbols of secondary faulting are scaled relative to those of primary faulting mechanism. Rectangles, normal faulting; batons, reverse faulting; crosses, strike-slip faulting.

per crust) the effect of fault continuity on slip rate may be the same for either elastic or anelastic models. For longer fault segments, however, slip rate is independent of segment length.

Aside from the step over regions, strain rate in the regions bounded by faults is primarily concentrated near fault bends. For example, off-fault strain rate increases near the bend of the San Andreas fault in the Santa Cruz Mountains (Plate 1b). The style of secondary faulting predicted by the model is reverse faulting aligned subparallel to the San Andreas fault in the Santa Cruz Mountains and the southern part of the San Francisco Peninsula, transitioning to N-S striking normal faulting near the Golden Gate. Except for the $M5.3$ 1957 Daly City earthquake the predicted pattern of deformation agrees well with focal mechanisms in the region determined by *Zoback et al.* [1999] and with mapped faults in the region. Note also that the sense of movement along the San Gregorio fault changes from oblique thrust faulting to oblique normal faulting near the Golden Gate (Plate 1a), the latter being consistent with offshore structural interpretations. The overall pattern of strain rate is sensitive to the surface heat flow distribution used to infer the lithospheric geotherm. More information and analysis of heat flow data in the San Francisco Bay area is needed to more accurately model the magnitude and pattern of long-term strain rates in the regions bounded by major faults.

4. Conclusions

Simulations of combined frictional-dislocation creep behavior of the continental lithosphere in northern California are able to explain the known slip rates of major faults with a low margin of error. We find that the quality of fits to stress orientation and fault slip rates is nearly independent of the viscous rheology of the lower crust. This is probably due to the rather large heat flow in the Coast Ranges of California, which makes the lower crust weak. Conversely, the broad Coast Range anomaly can be explained by ductile shear heating in the lower crust that is driven by movement of a strong upper crust (model 1 of *Thatcher and England* [1998]). Deformation of the upper crust in this region therefore is determined primarily by stress in the upper crust and not by stresses in a strong lower crust/mantle transferred to the upper crust. More information on the thermal structure in the San Francisco Bay region is needed toward delineating the lateral extent of heat flow anomalies and detailed deformation trends in the region.

A second conclusion is that major faults must have significantly lower coefficient of friction than the internal friction off the faults in the upper crust. Model results indicate that the apparent coefficient of friction on all of the major faults is less than 0.15, in agreement with the low strength of major faults in central and southern California determined in the previ-

ous study by *Bird and Kong* [1994]. A lower as well as an upper bound for San Andreas fault friction is indicated by the prediction error estimates such that $0.11 > \mu_{SAF} > 0.08$. Small gaps between modeled fault segments have only a small effect on slip rates. Continuum deformation in a gap represents subsidiary faulting, which, although it occurs at higher friction, allows continuity of slip through the irregularity in the fault system.

Deformation is easiest if blocks of the upper crust between major fault segments can move as rigid bodies. This is not possible with fault branches that are not straight and parallel, unless the faults have a nonvertical dip. A dipping fault can accommodate convergence or divergence between blocks. Although we are modeling a fault system that is primarily strike-slip with vertical dip, the parameter to which slip rates and stress orientations are most sensitive is dip of the faults. The bend in the San Andreas fault north of Point Arena is a strong impediment to slip, unless the fault has a nonvertical dip there. The correct partition of slip between the San Andreas and eastern fault strands is found only when normal faulting is allowed in the bend, as is suggested by marine seismic surveys. On the other hand, we find that a nonvertical dip on the Santa Cruz Mountains segment of the San Andreas allows that segment to slip too freely. A near-vertical dip is needed there to produce compressive stress and transfer slip to the San Gregorio fault.

Although there is generally a good agreement between slip rates predicted by the model and geologic estimates, discrepancies include a higher than expected slip rate on the Peninsula segment of the San Andreas fault and a slightly lower than expected slip rate on the San Gregorio fault. These model results, however, agree with slip partitioning at this latitude presented by *Argus and Gordon* [2000]. Off-fault patterns of deformation also seem to agree with geologic mapping of recent faulting and focal mechanisms, particularly in the regions of the San Francisco Peninsula, Santa Cruz Mountains, and Golden Gate platform [*Zoback et al.,* 1999].

References

Anderson, E. M., *The Dynamics of Faulting,* 206 pp., Oliver and Boyd, White Plains, N. Y., 1951.

Argus, D. F., and R. G. Gordon, Present tectonic motion across the Coast Ranges and San Andreas fault system in central California, *Geol. Soc. Am. Bull.,* in press, 2000.

Beaudoin, B. C., *et al.,* Transition from slab to slabless: Results from the 1993 Mendocino triple junction seismic experiment, *Geology, 24,* 195-199, 1996.

Bilham, R., and P. Bodin, Fault zone connectivity: Slip rates on faults in the San Francisco Bay Area, California, *Science, 258,* 281-284, 1992.

Bird, P., Stress and temperature in subduction shear zones: Tonga and Mariana, *Geophys. J. R. Astron. Soc., 55,* 411-434, 1978.

Bird, P., New finite element techniques for modeling deformation histories of continents with stratified temperature-dependent rheology, *J. Geophys. Res., 94,* 3967-3990, 1989.

Bird, P., Computer simulations of Alaskan neotectonics, *Tectonics, 15,* 225-236, 1996.

Bird, P., and X. Kong, Computer simulations of California tectonics confirm very low strength of major faults, *Geol. Soc. Am. Bull., 106,* 159-174, 1994.

Borchardt, G., D. L. Snyder, and C. J. Wills, Holocene slip rate of the Concord fault at Galindo Creek in Concord, California, final technical report, contract 1434-HQ-97-GR-03102, 30 pp., U.S. Geol. Surv., Menlo Park, Calif., 1999.

Brocher, T. M., J. McCarthy, P. E. Hart, W. S. Holbrook, K. P. Furlong, T. V. McEvilly, J. A. Hole and S. L. Klemperer, Seismic evidence for a lower-crustal decollement beneath San Francisco bay, California, *Science, 265,* 1436-1439, 1994.

Budding, K. E., D. P. Schwartz, and D. H. Oppenheimer, Slip rate, earthquake recurrence, and seismogenic potential of the Rodgers Creek fault zone, northern California: Initial results, *Geophys. Res. Lett., 18,* 447-450, 1991.

Byerlee, J., Friction, overpressure, and fault normal compression, *Geophys. Res. Lett., 17,* 2109-2112, 1990.

Ellis, S., P. Fullsack, and C. Beaumont, Oblique convergence of the crust driven by basal forcing: implications for length-scales of deformation and strain partitioning in orogens, *Geophys. J. Int., 120,* 24-44, 1995.

England, P. C., and D. P. McKenzie, A thin viscous sheet model for continental deformation, *Geophys. J. R. Astron. Soc., 70,* 295-321, 1982.

Geist, E. L., Relationship between the present-day stress field and plate boundary forces in the Pacific Northwest, *Geophys. Res. Lett., 23,* 3381-3384, 1996.

Geist, E. L., and D. W. Scholl, Large-scale deformation related to the collision of the Aleutian arc with Kamchatka, *Tectonics, 13,* 538-560, 1994.

Geist, E. L., M. A. Fisher, and D. W. Scholl, Large-scale deformation associated with ridge subduction, *Geophys. J. Int., 155,* 344-366, 1993.

Hall, N. T., T. D. Hunt, and P. R. Vaughan, Holocene behavior of the San Simeon fault zone, south-central coastal California, in *Seismotectonics of the Central California Coast Ranges,* edited by I. B. Alterman *et al.,* Spec. Pap. Geol. Soc. Am., 292, 167-189, 1994.

Hall, N. T., R. H. Wright, and K. B. Clahan, Paleoseismic studies of the San Francisco peninsula segment of the San Andreas fault zone near Woodside, California, *J. Geophys. Res., 104,* 23,215-23,236, 1999.

Hill, D. P., J. P. Eaton, W. L. Ellsworth, R. S. Cockerham, F. W. Lester, and E. J. Corbett, The seismotectonic fabric of central California, in *Neotectonics of North America, Decade Map Vol. 1,* edited by D. B. Slemmons *et al.,* pp. 107-132, Geol. Soc. Am., Boulder, Colo., 1991.

Hole, J. A., B. C. Beaudoin, and T. J. Henstock, Wide-angle seismic constraints on the evolution of the deep San Andreas plate boundary by Mendocino triple junction migration, *Tectonics, 17,* 802-818, 1998.

Houseman, G., and P. England, Finite strain calculations of continental deformation, 1, Method and general results for convergent zones, *J. Geophys. Res., 91,* 3651-3663, 1986.

Kelson, K. I., G. D. Simpson, W. R. Lettis, and C. C. Ha-

raden, Holocene slip rate and recurrence of the northern Calaveras fault at Leyden Creek, eastern San Francisco Bay region, *J. Geophys. Res., 101,* 5961-5975, 1996.

Kirby, S. H., and A. K. Kronenberg, Rheology of the lithosphere: Selected topics, *Rev. Geophys., 25,* 1219-1244, 1987.

Lachenbruch, A. H., and J. H. Sass, Heat flow and energetics of the San Andreas fault zone, *J. Geophys. Res., 85,* 6185-6222, 1980.

Lachenbruch, A. H., and J. H. Sass, Heat flow from Cajon pass, fault strength, and tectonic implications, *J. Geophys. Res., 97,* 4995-5015, 1992.

Lienkaemper, J. J., and G. Borchardt, Holocene slip rate of the Hayward fault at Union City, California, *J. Geophys. Res., 101,* 6099-6108, 1996.

McCulloch, D. S., Regional geology and hydrocarbon potential of offshore central California, in *Geology and Resource Potential of the Continental Margin of Western North America and Adjacent Ocean Basins: Beaufort Sea to Baja California, Earth Sci. Ser.,* vol. 6, edited by D. W. Scholl, A. Grantz, and J. G. Vedder, pp. 353-401, Circum-Pac. Counc. for Energy and Miner. Resour., Houston, Tex., 1987.

Mount, V. S., and J. Suppe, State of stress near the San Andreas fault: Implications for wrench tectonics, *Geology, 15,* 1143-1146, 1987.

Nábèlek, J. L., Downdip geometry of the Loma Prieta rupture from teleseismic waveform inversion, in *The Loma Prieta, California, Earthquake of October 17, 1989: Main Shock Characteristics,* edited by P. Spudich, *U.S. Geol. Surv. Prof. Pap., 1550-A,* 171-182, 1996.

Niemi, T. M., and N. T. Hall, Late Holocene slip rate and recurrence of great earthquakes on the San Andreas fault in northern California, *Geology, 20,* 195-198, 1992.

Parsons, T., Seismic-reflection evidence that the Hayward fault extends into the lower crust of the San Francisco Bay area, California, *Bull. Seismol. Soc. Am., 88,* 1212-1223, 1998.

Prentice, C. S., Earthquake geology of the northern San Andreas fault near Point Arena, California, Ph.D. thesis, 252 pp., Calif. Inst. of Tech., Pasadena, 1989.

Prentice, C. S., D. J. Merritts, E. C. Beutner, P. Bodin, A. Schill, and J. R. Muller, Northern San Andreas fault near Shelter Cove, California, *Geol. Soc. Am. Bull., 111,* 512-523, 1999.

Robertson, E. C., Continuous formation of gouge and breccia during fault displacement, in *Issues in Rock Mechanics,* edited by R. E. Goodman and F. E. Heuze, pp. 397-404, Soc. of Min. Eng. Am. Inst. of Min., Metal., and Pet. Eng., New York, 1982.

Thatcher, W., and P. C. England, Ductile shear zones beneath strike-slip faults: Implications for the thermomechanics of the San Andreas fault zone, *J. Geophys. Res., 103,* 891-905, 1998.

Tse, S. T., R. Dmowska, and J. R. Rice, Stressing of locked patches along a creeping fault, *Bull. Seismol. Soc. Am., 75,* 709-736, 1985.

Turcotte, D. L., P. H. Tag, and R. F. Cooper, A steady-state model for the distribution of stress and temperature on the San Andreas fault, *J. Geophys. Res., 85,* 6224-6230, 1980.

Ward, S. N., Dogtails versus rainbows: Synthetic earthquake rupture models as an aid in interpreting geological data, *Bull. Seismol. Soc. Am., 87,* 1422-1441, 1997.

Wdowinski, S., R. J. O'Connell, and P. England, A continuum model of continental deformation above subduction zones: Application to the Andes and the Aegean, *J. Geophys. Res., 94,* 10,331-10,346, 1989.

Weber, G. E., and J. M. Nolan, Determination of late

Pleistocene-Holocene slip rates along the San Gregorio fault zone, San Mateo County, California, *U.S. Geol. Surv. Open File Rep., 95-210*, 805-807, 1995.

Working Group on Northern California Earthquake Potential (WGNCEP), Database of potential sources for earthquakes larger than magnitude 6 in northern California, *U.S. Geol. Surv. Open File Rep., 96-705*, 53 pp., 1996.

Zoback, M. D., and M. L. Zoback, Tectonic stress field of North America, in *Neotectonics of North America, Decade Map Vol. 1,* edited by D. B. Slemmons, *et al.*, pp. 339-366, Geol. Soc. of Am., Boulder, Colo., 1991.

Zoback, M. D., *et al.*, New evidence on the state of stress of the San Andreas fault system, *Science, 238,* 1105-1111, 1987.

Zoback, M. L., R. C. Jachens, and J. A. Olson, Abrupt along-strike change in tectonic style: San Andreas fault zone, San Francisco peninsula, *J. Geophys. Res., 104,* 10,719-10,742, 1999.

E. L. Geist and D. J. Andrews, U.S. Geological Survey, 345 Middlefield Road, MS 999, Menlo Park, CA 94025. (geist@octopus.wr.usgs.gov; jandrews@usgs.gov)